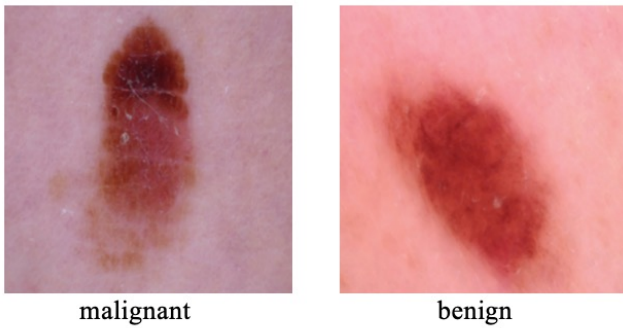In Section 7, we provide additional details on datasets (ISIC (7.1), HCDD (7.2) and NIH (7.3)).
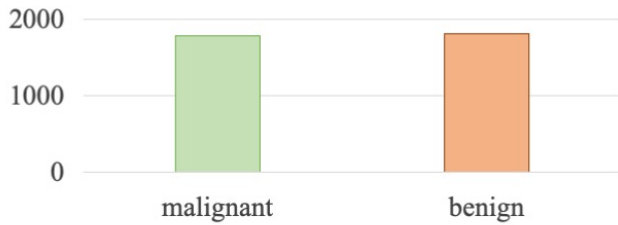
7 MORE DETAILS ON THE DATASETS

7.1 Description of the ISIC Dataset.

To further demonstrate ISIC dataset, we present additional visualization images about the four categories. As can be seen in Fig 7, ISIC is classified as: malignant (1782 images) and benign (1800 images). Although the ISIC classes are similar, our algorithm still achieves a good performance.

(a) Schematic diagram of the classes of ISIC
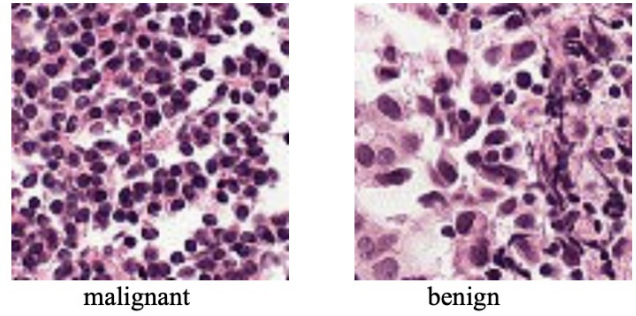

(b) Illustration of the number of categories

Figure 7: Illustration of BraTS dataset. (a) BraTS dataset with four Categories. (b) Imbalanced class distribution of BraTS dataset.
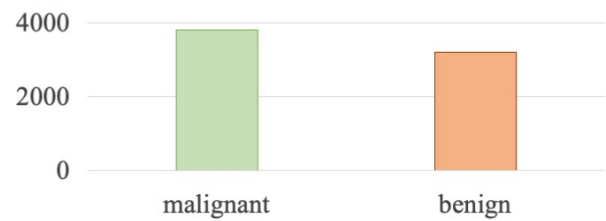
7.2 Description of the MNIST Dataset.

For the Kaggle histopathologic cancer detection dataset (HCDD), as can be seen in Fig 8, the dataset is a binary classification for malignant and benign, containing low-resolution images of lymph node sections with about 30, 0000 markers extracted from digital histopathological scans. We randomly select 6200 and 800 images from the training images as our training data and test data, respectively. These results on HCDD dataset further demonstrate the generalizability of our **Pseudo-T correction**, which still performs well on the HCDD dataset.

7.3 Description of the NIH Dataset.

For a more visual presentation of NIH dataset, we show the 14 categories of this dataset. As can be seen in Fig. 9, NIH is classified
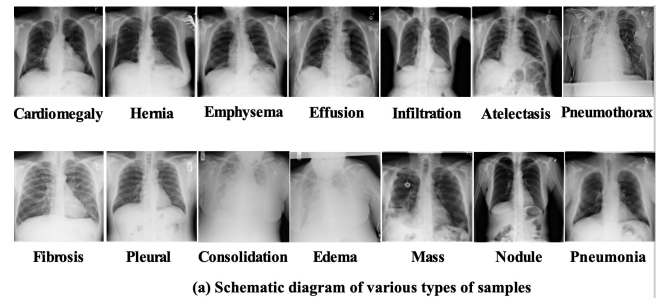

(a) Schematic diagram of the classes of HCDD

(b) Illustration of the number of categories

Figure 8: Illustration of our samples. (a)MNIST dataset with clean and corrupted samples. Red labels mean noisy labels. (b) Imbalanced class distribution of MNIST dataset.

(a) Schematic diagram of various types of samples

(b) Statistical schematic of the number of different categories in NIH dataset

Figure 9: Illustration of NIH dataset.

as: Cardiomegaly, Hernia, Emphysema, Effusion, Infiltration, Atelectasis, Pneumothorax, Fibrosis, Pleural, Consolidation, Edema, Mass, Nodule and Pneumonia.